



**HAL**  
open science

## **Mycobacterium tuberculosis H37Rv parietal and cellular lipoarabinomannans. Characterization of the acyl- and glyco-forms.**

M. Gilleron, L. Bala, T. Brando, Alain Vercellone, G. Puzo

### ► To cite this version:

M. Gilleron, L. Bala, T. Brando, Alain Vercellone, G. Puzo. Mycobacterium tuberculosis H37Rv parietal and cellular lipoarabinomannans. Characterization of the acyl- and glyco-forms.. Journal of Biological Chemistry, 2000, 275 (1), pp.677-84. hal-00177657

**HAL Id: hal-00177657**

**<https://hal.science/hal-00177657>**

Submitted on 22 Mar 2021

**HAL** is a multi-disciplinary open access archive for the deposit and dissemination of scientific research documents, whether they are published or not. The documents may come from teaching and research institutions in France or abroad, or from public or private research centers.

L'archive ouverte pluridisciplinaire **HAL**, est destinée au dépôt et à la diffusion de documents scientifiques de niveau recherche, publiés ou non, émanant des établissements d'enseignement et de recherche français ou étrangers, des laboratoires publics ou privés.

# *Mycobacterium tuberculosis* H37Rv Parietal and Cellular Lipoarabinomannans

CHARACTERIZATION OF THE ACYL- AND GLYCO-FORMS\*

(Received for publication, May 20, 1999, and in revised form, October 4, 1999)

Martine Gilleron‡, Lakshmi Bala§, Thérèse Brando, Alain Vercellone¶, and Germain Puzo

From the Institut de Pharmacologie et de Biologie Structurale du Centre National de la Recherche Scientifique, 205 route de Narbonne, 31077 Toulouse Cedex, France

**Mannosylated lipoarabinomannans are multifaceted molecules. They have been shown to exert an immunosuppressive role in the immunopathogenesis of tuberculosis. They are also described as antigens of host double negative  $\alpha\beta$  T-cells. Delimitation of ManLAMs epitopes require knowledge of the precise structure of these molecules. The two major functional domains (the cap motifs and the phosphatidylinositol anchor) of the parietal and cellular ManLAMs of *Mycobacterium tuberculosis* H37Rv were investigated here. Using capillary electrophoresis, we established that parietal and cellular ManLAMs share the same capping motifs, mono-, di-, and trimannosyl units with the same relative abundance. By  $^{31}\text{P}$  NMR analysis of the native LAMs in  $\text{Me}_2\text{SO}-d_6$ , the major acyl-form of both parietal and cellular H37Rv ManLAM anchors, typified by the P3 phosphorus resonance, comprised a diacylglycerol unit. Three other acyl-forms were characterized in the cellular ManLAMs. Comparative analysis of the cellular *Mycobacterium bovis* BCG and *M. tuberculosis* ManLAM acyl-forms revealed the presence of the same populations, but with different relative abundance. The biological importance of the H37Rv ManLAM acyl-form characterization is discussed, particularly concerning the molecular mechanisms of binding of ManLAMs to the CD1 proteins involved in the presentation of ManLAMs to T-cell receptors.**

The highly immunogenic lipoglycans ubiquitously found in the mycobacterial envelope, the lipoarabinomannans (LAMs)<sup>1</sup> (1, 2), are thought to play a major role in the immunopathogenesis of tuberculosis. They regulate cytokine secretion (3–

10), block the transcriptional activation of interferon- $\gamma$  (10), and neutralize the potentially cytotoxic oxygen free radicals (11). Mannosylated LAMs (ManLAMs) selectively bind murine and human macrophages via the mannose receptor (12, 13) and have been found to stimulate CD4/CD8 double negative and CD8  $\alpha\beta$ T cells restricted by CD1 molecules (14).

It is now well established that LAMs, irrespective of their source, are heterogeneous in size. This was first revealed by SDS-polyacrylamide gel electrophoresis analysis where LAMs migrate as broad band around 30–40 kDa (15). The LAM molecular weight was more precisely determined using matrix-assisted laser desorption ionization-time of flight mass spectrometry. Indeed, it was found that LAMs are macromolecules of around 17 kDa with a size distribution of at least 4 kDa (16). Thus, any structural feature or biological parameter will be a weighted average of the composite molecular species.

In an attempt to improve the purification of the *Mycobacterium bovis* BCG LAMs, we developed a new extraction procedure leading to two pools of ManLAMs, namely parietal and cellular (17). Structurally, these ManLAMs differ mainly in the structure of the phosphatidyl-*myo*-inositol anchor lipid moiety and the percentage of manno-oligosaccharide caps (9). The parietal ManLAM anchor corresponds to one acyl-form, characterized by acylation of the OH-1 of the glycerol residue by 12-*O*-(methoxypropanoyl)-12-hydroxystearic acid, a novel fatty acid in the *Mycobacterium* genus, while the anchor of the cellular ManLAMs exhibited a higher degree of acylation from a combination of palmitic and tuberculostearic acids. In addition, these two pools of ManLAMs were found to stimulate interleukin-8 and tumor necrosis factor- $\alpha$  secretion from human dendritic cells to different extents (9).

We report here an elucidation of structural features of the ManLAMs isolated from *Mycobacterium tuberculosis* H37Rv. Previous studies on the parietal LAMs (16) and on the total LAM fraction (18) from *M. tuberculosis* H37Rv cells demonstrated that they belong to the ManLAMs class. The degree of mannose capping has been estimated, from the total ManLAM fraction, to be around 40% (19).

The new extraction protocol developed for *M. bovis* BCG (9) enabled isolation from *M. tuberculosis* H37Rv of two pools of LAMs, namely parietal and cellular. Their two major functional domains were characterized as follows: (i) the cap motifs by capillary electrophoresis, (ii) the phosphatidyl-*myo*-inositol anchor by NMR spectroscopy.

## EXPERIMENTAL PROCEDURES

*M. tuberculosis* H37Rv ManLAMs Extraction and Purification—Parietal and cellular ManLAMs were purified as described by Nigou *et al.* (9). Briefly, *M. tuberculosis* H37Rv cells were delipidated using  $\text{CHCl}_3/\text{CH}_3\text{OH}$ , 1:1 (v/v). The delipidated mycobacteria were extracted six times by refluxing in 50% ethanol at 65 °C for 8 h (parietal pool). The resulting cells (cellular pool) were washed and disintegrated in ice by

\* This work was supported by grants from the Région Midi-Pyrénées, pôle agroalimentaire (RECH/9702343), the Ministère de l'Éducation Nationale, de la Recherche et des Technologies (MENRT Microbiologie, 9710047). The costs of publication of this article were defrayed in part by the payment of page charges. This article must therefore be hereby marked "advertisement" in accordance with 18 U.S.C. Section 1734 solely to indicate this fact.

‡ To whom correspondence should be addressed. Tel.: 33-5-61-17-55-04; Fax: 33-5-61-17-59-94; E-mail: gilleron@ipbs.fr.

§ Present address: Div. of Membrane Biology, Central Drug Research Institute, Chhataramanzil, PB 173, Lucknow 226 001, India.

¶ Present address: Unité 395-CHU Purpan, BP 3028, 31028 Toulouse Cedex, France.

<sup>1</sup> The abbreviations used are: LAMs, lipoarabinomannans; AMs, arabinomannans; BCG, bacillus Calmette Guérin; CD1, cluster of differentiation I; GC/MS, gas chromatography/mass spectrometry; HMQC, heteronuclear multiple quantum correlation spectroscopy; HOHAHA, homonuclear Hartmann-Hahn spectroscopy; ManAMs, AMs with mannosyl extensions; ManLAMs, LAMs with mannosyl extensions; LMs, lipomannans; <sup>1</sup>H, <sup>13</sup>C, and <sup>31</sup>P NMR, proton, carbon, and phosphorus nuclear magnetic resonance; Man<sub>p</sub>, mannopyranosyl unit; Ara<sub>f</sub>, arabinofuranosyl unit; *myo*-Ins: *myo*-inositol; Gro, glycerol; t, terminal.

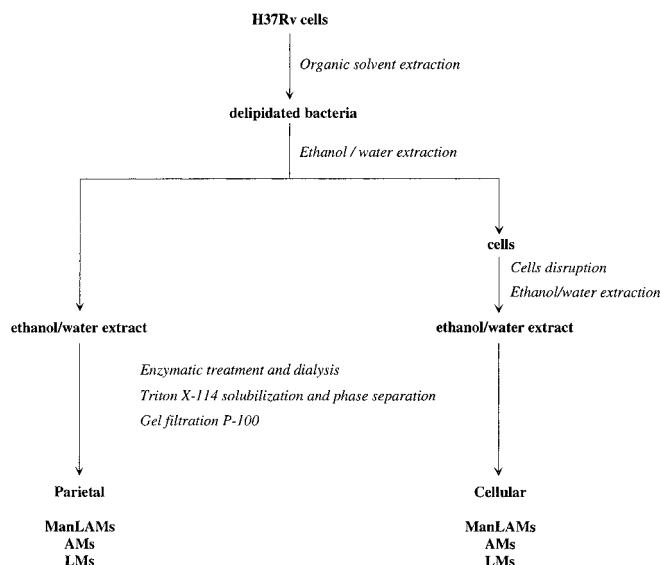


FIG. 1. Purification scheme for the parietal and cellular ManLAMs and related compounds (AMs and LMs) from *M. tuberculosis* H37Rv.

sonication and using a French pressure cell as described previously (9). Each parietal and cellular extract was treated to remove proteins, phosphatidyl-*myo*-inositol mannosides, DNA, RNA, and glucose leading to glycanic- and lipoglycanic-rich extracts. Both extracts were subjected to Triton X-114 phase separation. ManLAMs and LMs were then separated by gel filtration, as described previously (9). The purified ManLAMs and LMs monitored by SDS-polyacrylamide gel electrophoresis were observed as broad bands around 35 and 20 kDa, respectively, as described by Venisse *et al.* (16).

**Acetolysis Procedure**—3 mg of ManLAMs were treated with 400  $\mu$ l of anhydrous acetic acid/acetic anhydride, 3:2 (v/v), at 110  $^{\circ}$ C for 12 h (20). The reaction mixture was dried and vortexed with 400  $\mu$ l of cyclohexane/water, 1:1 (v/v). The cyclohexane phase which contains the acylglycerol residues was analyzed by GC/MS, as described previously (9).

**GC and GC/MS Analysis**—GC was performed on a Girdel series 30 chromatograph equipped with an OV1 capillary column (0.22 mm  $\times$  25 m) using helium gas with a flow rate of 2.5 ml/min and a flame ionization detector at 310  $^{\circ}$ C. The injector temperature was 260  $^{\circ}$ C and the temperature separation program was from 100 to 290  $^{\circ}$ C rising at 3  $^{\circ}$ C/min. GC/MS analysis were performed on a Hewlett-Packard 5889X mass spectrometer (electron energy, 70 eV) working in both electron impact and chemical ionization modes using  $\text{NH}_3$  as reagent gas coupled with a Hewlett-Packard 5890 gas chromatograph series II fitted with a similar OV1 column (0.30 mm  $\times$  12 m). Acetolysis products were analyzed on a 0.35-m length column using a temperature separation program from 160 to 300  $^{\circ}$ C at 8  $^{\circ}$ C/min. The injector and interface temperatures were 290  $^{\circ}$ C.

**Capillary Electrophoresis**—Analyses were performed on a P/ACE capillary electrophoresis system (Beckman Instruments, Inc.) with the cathode on the injection side and the anode on the detection side. The electropherograms were acquired and stored on a Dell XPS P60 computer using the System Gold software package (Beckman Instruments, Inc.).

Two micrograms of dried mild hydrolyzed (0.1 N HCl at 110  $^{\circ}$ C for 30 min) ManLAMs were mixed with 0.5  $\mu$ l of 0.2 M 1-aminopyrene-3,6,8-trisulfonate (APTS) (eCAP N-linked Oligosaccharides Profiling kit; Beckman) in 15% acetic acid and 0.5  $\mu$ l of a 1 M sodium cyanoborohydride solution dissolved in tetrahydrofuran (Aldrich) (21). The reaction was 90 min at 55  $^{\circ}$ C and the samples were then diluted in 9  $\mu$ l of water before injection. APTS derivatives were loaded by applying a 0.5 p.s.i. (3.45 kilopascal) vacuum for 5 s. The derivatives were separated on a coated capillary column (eCAP N-CHO Coated Capillary from eCAP N-linked Oligosaccharides Profiling kit; Beckman) of 50- $\mu$ m internal diameter with 40-cm effective length (47 cm total length). Analyses were carried out at a temperature of 20  $^{\circ}$ C with an applied voltage of 24 kV using degassed Carbohydrate Separation Gel buffer (eCAP N-linked Oligosaccharides Profiling kit; Beckman) as running electrolyte. The detection system consisted of a Beckman laser-induced fluorescence equipped with a 4-mW argon-ion laser with the excitation wavelength of 488 nm and emission wavelength filter of 520 nm.

TABLE I  
Proton and carbon chemical shifts from parietal ManLAMs of *M. tuberculosis* H37Rv dissolved in  $\text{Me}_2\text{SO}-d_6$

	1	2	3	4	5	6
I, 3,5- $\alpha$ -Araf	109.1 4.88	81.0 4.03	83.4 3.91	83.4 3.87	67.7 3.60/3.74	
II, 5- $\alpha$ -Araf	109.0 4.83 109.1 4.85 108.0 4.99	82.4 3.88 82.5 3.88 82.8 3.88	78.2 3.75 78.4 ND 78.2 3.78	82.8 3.93 ND <sup>a</sup> ND ND ND	67.7 3.69/3.58 ND ND 67.7 3.71/3.58	
III, 2- $\alpha$ -Araf	106.7 4.98 106.6 4.99 106.1 5.11	88.4 4.00 88.6 4.00 88.8 3.99	76.1 3.89 ND 3.92 ND 3.89	84.25 3.85 ND 3.88 ND 3.81	62.0 3.63/3.50 ND 3.63/3.51 ND 3.63/3.51	
IV, <i>t</i> - $\alpha$ -Manp	102.9 4.91 102.9 4.92	70.8 3.78 70.95 3.82	71.8 ND 71.8 3.59	68.2 3.44 68.0 3.50	ND 3.51 74.3 3.55	3.69 62.1 3.70/3.53
V, $\beta$ -Araf	101.8 4.94 101.5 5.09	77.7 3.86 77.6 3.90	76.3 3.83 ND ND	81.4 3.78 ND ND	70.0 3.71/3.56 ND ND	
VI, 6- $\alpha$ -Manp	100.4 4.71	70.95 3.71	72.0 3.56	ND 3.62	ND 3.52	66.7 3.74/3.63
VII, 2- $\alpha$ -Manp	99.3 4.87	78.3 3.76	71.3 3.68	68.2 3.45	74.8 3.52	ND ND
VIII, 2,6- $\alpha$ -Manp	99.2 4.90	78.75 3.80	71.4 3.73	67.6 3.61	72.5 3.61	66.7 3.84/3.52

<sup>a</sup> ND, not determined.

**NMR Spectroscopy**—Prior to NMR spectroscopic analysis, the parietal (12.8 mg) and cellular (15 mg) ManLAM fractions were exchanged in  $\text{D}_2\text{O}$  (99.9% purity) at room temperature with intermediate freeze-drying, and then dissolved in 400  $\mu$ l of  $\text{Me}_2\text{SO}-d_6$  (99.8% purity, Eurisotop, Saint Aubin, France). The samples were analyzed in 200  $\times$  5-mm 535-PP NMR tubes at 70  $^{\circ}$ C on a Bruker DMX-500 500 MHz NMR spectrometer equipped with a double resonance ( $^1\text{H}/\text{X}$ )-BBi z-gradient probe head. Proton and carbon chemical shifts are expressed in parts/million downfield from the methyl of  $\text{Me}_2\text{SO}-d_6$  ( $\delta_{\text{H}}$ /trimethylsilyl 2.52 and  $\delta_{\text{C}}$ /trimethylsilyl 40.98). The one-dimensional phosphorus ( $^{31}\text{P}$ ) spectra were measured at 202.46 MHz and phosphoric acid (85%) was used as the external standard ( $\delta_{\text{P}}$  0.0). All two-dimensional NMR data sets were recorded without sample spinning and data were acquired in the phase-sensitive mode using the time-proportional phase increment method (22). Four two-dimensional Homonuclear Hartmann-Hahn (HOHAHA) spectra were recorded using MLEV-17 mixing sequences of 9, 43, 82, and 113 ms (23). The  $^1\text{H}-^{13}\text{C}$  and  $^1\text{H}-^{31}\text{P}$  single-bond correlation spectra (HMQC) were obtained using Bax's pulse sequence (24). The GARP sequence (25) at the carbon or phosphorus frequency was used as a composite pulse decoupling during acquisition. The pulse sequence used for  $^1\text{H}$ -detected heteronuclear relayed spectra (HMQC-HOHAHA) was that of Lerner and Bax (26).

Standards (1,2-diacyl-3-phospho-*sn*-glycerol, *sn*-glycero-3-phospho-(1-*D*-*myo*-inositol), and *L*- $\alpha$ -lysophosphatidylinositol) were purchased from Sigma. *L*- $\alpha$ -Lysophosphatidylinositol, *i.e.* monoacyl-*sn*-glycero-3-phospho-(1-*D*-*myo*-inositol) standard, was a mixture of approximately 82% 1-acyl-2-lyso-*sn*-glycero-3-phospho-(1-*D*-*myo*-inositol) (by integration of the  $^{31}\text{P}$  signal at 5.39 ppm obtained in  $\text{Me}_2\text{SO}-d_6$  at 343 K) and 18% 1-lyso-2-acyl-*sn*-glycero-3-phospho-(1-*D*-*myo*-inositol) ( $^{31}\text{P}$  signal at 4.94 ppm).

## RESULTS

Using a new extraction method (17), two pools of LAMs, called parietal and cellular, were isolated from the envelope of *M. bovis* BCG. This method was applied to the H37Rv cells (Fig. 1) and enabled recovery of 88 mg of parietal and 135 mg

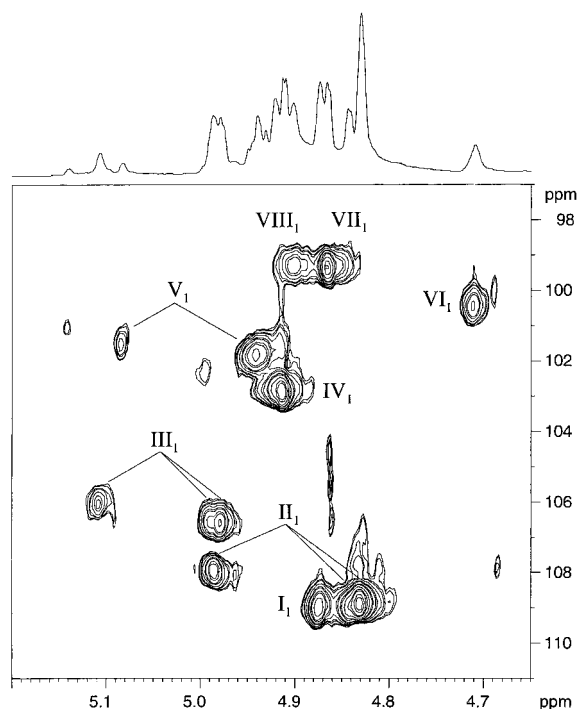


FIG. 2. Expanded region ( $\delta^1\text{H}$ : 4.65–5.20,  $\delta^{13}\text{C}$  97–111) of the two-dimensional  $^1\text{H}$ - $^{13}\text{C}$  HMQC spectrum in  $\text{Me}_2\text{SO}-d_6$  at 343 K of *M. tuberculosis* H37Rv cellular ManLAMs. I, 3,5- $\alpha$ -Araf; II, 5- $\alpha$ -Araf; III, 2- $\alpha$ -Araf; IV, *t*- $\alpha$ -Manp; V,  $\beta$ -Araf; VI, 6- $\alpha$ -Manp; VII, 2- $\alpha$ -Manp; VIII, 2,6- $\alpha$ -Manp.

of cellular LAMs. Their capping motifs and their anchor domains were then characterized.

**Structure of the Manno-oligosaccharide Caps**—Parietal and cellular *M. bovis* BCG LAMs were shown to belong to the ManLAM class by two-dimensional  $^1\text{H}$ - $^{13}\text{C}$  HMQC study on LAMs dissolved in  $\text{D}_2\text{O}$  (17, 27). Indeed, the anomeric protons of *t*-Manp and 2-*O*-linked Manp from the mannan core and the manno-oligosaccharide caps resonate independently, corresponding to four independent spin systems. However, an improved resolution in the  $^1\text{H}$  and  $^{31}\text{P}$  spectra was obtained by dissolving the multiacylated ManLAMs (28) and LMs (29) of *M. bovis* BCG in  $\text{Me}_2\text{SO}-d_6$ . H37Rv LAMs were then analyzed in  $\text{Me}_2\text{SO}-d_6$  by a complete NMR strategy involving two-dimensional  $^1\text{H}$ - $^1\text{H}$  COSY, HOHAHA with different mixing times,  $^1\text{H}$ - $^{13}\text{C}$  HMQC and  $^1\text{H}$ - $^{13}\text{C}$  HMQC-HOHAHA in order to characterize the different spin systems which compose the LAMs. This was conducted with help of the complete NMR analysis of the mannan core of the parietal ManAMs carried out in  $\text{D}_2\text{O}$  (30) and the ManLAMs from *M. bovis* BCG<sup>2</sup> and of the data obtained in  $\text{Me}_2\text{SO}-d_6$  on the *M. bovis* BCG LMs (29). In this respect, 14 spin systems were highlighted, assigned as 9 types of Araf (1 type of 3,5- $\alpha$ -Araf, 3 types of 5- $\alpha$ -Araf, 3 types of 2- $\alpha$ -Araf, and 2 types of  $\beta$ -Araf) and 5 types of Manp (2 types of *t*- $\alpha$ -Manp, 1 type of 2- $\alpha$ -Manp, 1 type of 6- $\alpha$ -Manp, and 1 type of 2, 6- $\alpha$ -Manp) (Table I).

Fig. 2 illustrates the anomeric expansion area of the HMQC spectrum recorded in  $\text{Me}_2\text{SO}-d_6$  from H37Rv cellular LAMs. The anomeric C-H pairs of *t*-Manp and 2-*O*-linked Manp were investigated to determine the H37Rv LAM class. We observed four anomeric C-H pairs, one at 99.2/4.90 ( $\text{VIII}_1$ ), one at 99.3/4.87 ( $\text{VII}_1$ ), and two with the same  $^{13}\text{C}$  chemical shift and close  $^1\text{H}$  chemical shifts at 102.9/4.91 and 102.9/4.92 ( $\text{IV}_1$ ). They were assigned as the anomeric C-H pairs of 2,6- $\alpha$ -Manp ( $\text{VIII}$ ), 2- $\alpha$ -Manp ( $\text{VII}$ ), and *t*- $\alpha$ -Manp ( $\text{IV}$ ) from the manno-oligosac-

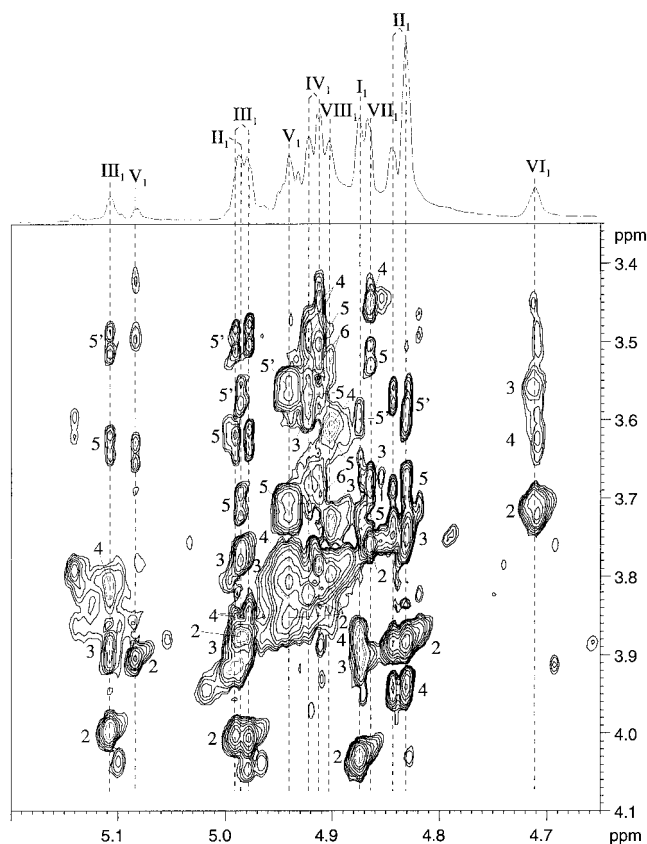


FIG. 3. Expanded region ( $\delta^1\text{H}$ , 4.65–5.20 and 3.35–4.10) of the two-dimensional 113 ms  $^1\text{H}$ - $^1\text{H}$  HOHAHA spectrum in  $\text{Me}_2\text{SO}-d_6$  at 343 K of *M. tuberculosis* H37Rv cellular ManLAMs. I, 3,5- $\alpha$ -Araf; II, 5- $\alpha$ -Araf; III, 2- $\alpha$ -Araf; IV, *t*- $\alpha$ -Manp; V,  $\beta$ -Araf; VI, 6- $\alpha$ -Manp; VII, 2- $\alpha$ -Manp; VIII, 2,6- $\alpha$ -Manp.

charide caps and the mannan core, respectively, by comparison to the NMR data obtained on the *M. bovis* BCG LMs (29). Indeed, LMs are less complex macromolecules as they are devoid of the arabinan domain. The mannan core structure has been characterized by NMR leading to the definition of the three main spin systems (2, 6- $\alpha$ -Manp, *t*- $\alpha$ -Manp, and 6- $\alpha$ -Manp) in terms of  $^1\text{H}$  and  $^{13}\text{C}$  chemical shifts (29). These three spin systems were retrieved in the LAMs NMR spectra allowing differentiation between the spin systems which belong to the mannan core and those which correspond to the manno-oligosaccharide caps present on the arabinan domain. Indeed, both *t*-Manp proton spin systems were clearly observed on the HOHAHA spectrum (Fig. 3), one from the H-1 at  $\delta$  4.91 and the other one from the H-1 at  $\delta$  4.92. In addition, the two  $^1\text{H}$  spin systems of the 2-*O*-linked Manp ( $\text{VII}$  and  $\text{VIII}$ ) assigned to 2- $\alpha$ -Manp and 2,6- $\alpha$ -Manp, respectively (Table I), were conspicuous in the HOHAHA spectrum (Fig. 3). Similar results were obtained for the parietal LAMs, demonstrating that parietal and cellular H37Rv LAMs belong to the ManLAM class.

The structures of these manno-oligosaccharide caps were then investigated by capillary electrophoresis analysis as described previously (9). Both parietal and cellular ManLAMs were submitted to: (i) mild acid hydrolysis, (ii) APTS tagging by reductive amination (21), and (iii) analysis by capillary electrophoresis monitored by laser-induced fluorescence. The electropherogram from the parietal ManLAMs after 30 min hydrolysis is shown in Fig. 4. The peaks were assigned from APTS standards and previous CE/ESI-MS studies concerning the structural elucidation of the manno-oligosaccharide caps from *M. bovis* BCG ManLAMs (9, 31). Peak I was assigned to free APTS reagent; peak II, which corresponds to the major compound,

<sup>2</sup> M. Gilleron, G. Nigou, and G. Puzo, unpublished data.

was Ara-APTS; peak III, Man-APTS; peak IV, Araf-Ara-APTS; peak V, Manp-Ara-APTS; peak VI, Manp-Manp-Ara-APTS; and finally peak VII, Manp-Manp-Manp-Ara-APTS. The latter compound was characterized by EC/ESI-MS analysis.<sup>3</sup> The extent of LAM hydrolysis was indicated by the relative intensities of peaks III and IV (Man-APTS and Araf-Ara-APTS, respectively). The relative abundance of the different caps was determined by integration of the peaks of interest (peaks V, VI, and VII), revealing that the major structural motif was the dimannosyl unit (66%), while the mannosyl and trimannosyl ones only represented 18 and 16%, respectively. Likewise, these manno-oligosaccharide cap structures, with the same relative abundance, were characterized for the cellular ManLAMs (not shown).

**Phosphatidyl-*myo*-Ins Anchor Acylation state**—The phosphatidyl-*myo*-Ins anchor structure was investigated from one-dimensional and two-dimensional phosphorus NMR. The one-dimensional <sup>31</sup>P spectra of the parietal and cellular ManLAMs exhibited broad unresolved signals in D<sub>2</sub>O (not shown) consistent with multiacylated ManLAMs (9, 28, 29). No connectivities between phosphate and protons could therefore be obtained by two-dimensional <sup>1</sup>H-<sup>31</sup>P HMQC and HMQC-HOHAHA. Recently, it was shown by Nigou *et al.* (28) that Me<sub>2</sub>SO-*d*<sub>6</sub> is a suitable solvent for recording high resolution one-dimensional <sup>31</sup>P NMR spectra of multiacylated ManLAMs. One-dimensional <sup>31</sup>P spectra of both H37Rv parietal (Fig. 5b) and cellular (Fig. 5c) ManLAMs dissolved in Me<sub>2</sub>SO-*d*<sub>6</sub> were thus recorded. The <sup>31</sup>P resonance were first assigned by comparison with the chemical shifts of the <sup>31</sup>P signals observed in the one-dimensional <sup>31</sup>P spectrum of the *M. bovis* BCG cellular ManLAMs (Fig. 5a) (28). The one-dimensional <sup>31</sup>P spectrum of the H37Rv parietal ManLAMs (Fig. 5b) showed one sharp resonance at δ 1.83 corresponding to P3, while, for the cellular ManLAMs, four signals at δ 1.66, δ 1.72, δ 1.83, and δ 3.50 were observed assigned to P1/P2/P3/P5, respectively (Fig. 5c). P1, P2, and P3 were tentatively assigned to ManLAMs containing a diacyl-Gro residue, while P5 corresponds to ManLAMs with a lyso-Gro residue. On the basis of the one-dimensional <sup>31</sup>P spectrum, it can be proposed that the H37Rv parietal ManLAMs comprise one acyl-form typified by diacyl-Gro residue, while at least three acyl-forms comprise the cellular ManLAMs. In addition, the relative abundance of the acyl-forms of the H37Rv cellular ManLAMs (Table III), determined from their signal heights, of

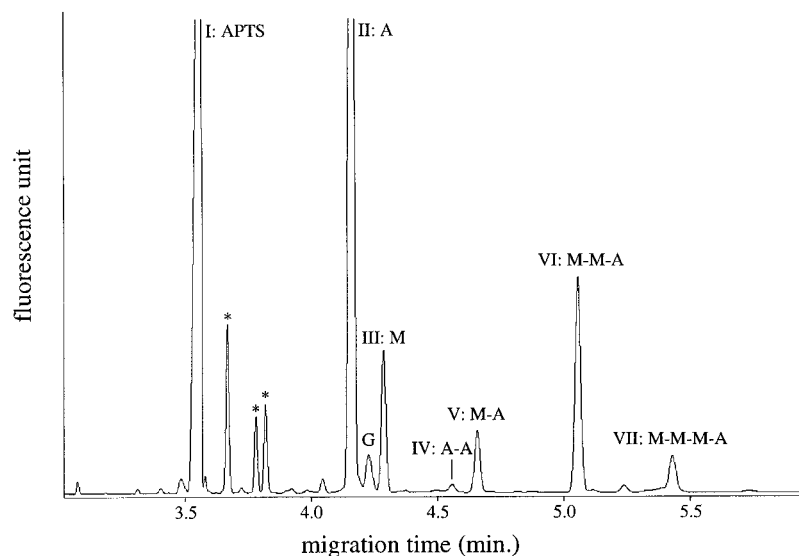
P1, 22%; P3, 67%; P4, 0%; P5, 11%, differed from those observed with the BCG ManLAMs (P1, 38%; P3, 42%; P4, 8%; P5, 12%). To further elucidate the structures of these anchors, two-dimensional <sup>1</sup>H-<sup>31</sup>P HMQC and HMQC-HOHAHA NMR experiments were conducted. The <sup>1</sup>H-<sup>31</sup>P HMQC-HOHAHA of parietal ManLAMs (Fig. 6a) exhibited one line of correlations for the P3 phosphate resonance. The HOHAHA spectrum (not shown) can discriminate between the Gro and the *myo*-Ins protons. From the H-5 at 3.10 ppm, the complete set of correlations of the *myo*-Ins proton spin system was assigned (δ<sub>H-1</sub> 4.02; δ<sub>H-2</sub> 4.11; δ<sub>H-3</sub> 3.24; δ<sub>H-4</sub> 3.45; δ<sub>H-6</sub> 3.59) from the coupling constants and chemical shifts. These chemical shifts were consistent with the absence of fatty acyl appendage on the *myo*-Ins. The Gro spin system defined from the <sup>1</sup>H-<sup>31</sup>P HMQC spectrum (H-3/H-3' 3.86/3.80 ppm) (Fig. 6b) and from the HOHAHA spectrum (H-1/H-1' at 4.36/4.14 ppm and H-2 at 5.12 ppm) corresponds to a diacylated Gro by reference to the standard 1,2-diacyl-3-phospho-*sn*-glycerol unit in Me<sub>2</sub>SO-*d*<sub>6</sub>: δ<sub>H-1/H-1'</sub> 4.33/4.13, δ<sub>H-2</sub> 5.10, δ<sub>H-3/H-3'</sub> 3.87/3.80.

The <sup>1</sup>H-<sup>31</sup>P HMQC-HOHAHA spectrum of cellular ManLAMs (Fig. 7a) exhibited a complex panel of correlations for P1, P3, and P5 phosphate resonance. P1 and P3 showed correlations with downfield resonances at δ 5.12 and 5.09 in *F*<sub>2</sub> dimension, which were assigned to methine protons H-2 of diacylated glycerol units according to previous results (28, 29). A similar downfield correlation was not observed in P5; instead the H-2 resonance is superimposed with the Gro H-3/H-3', indicating lack of acylation of O-2 in this minor species (see below). So, only P1 and P3 correspond to 1,2-diacyl-3-phospho-*sn*-glycerol units.

From the H-2 Gro resonance, each glycerol spin system corresponding to P1 and P3 was defined (Table II) from inspection of the HOHAHA spectrum (Fig. 7d). Likewise, the *myo*-Ins spin systems were identified (Table II) from the correlations lines of both H-5 at δ 3.18 (P1) and 3.11 (P3) (in *F*<sub>1</sub> dimension) in the HOHAHA spectrum (Fig. 7c) in comparison with previous results (28, 29) and from the multiplicity of the signals and the <sup>3</sup>*J*<sub>HH</sub> coupling constants. The two *myo*-Ins chemical shifts were relatively different. The P3 *myo*-Ins was assigned to a non-acylated phospho-*myo*-Ins by comparison with a standard (*sn*-glycero-3-phospho-(1-D-*myo*-inositol), δ<sub>H-1</sub> 3.65 (pd), δ<sub>H-2</sub> 3.88 (ps), δ<sub>H-3</sub> 3.18 (pd), δ<sub>H-4</sub> 3.44 (t), δ<sub>H-5</sub> 2.99 (t), δ<sub>H-6</sub> 3.66 (t); pd, pseudodoublet, ps, pseudosinglet, t, triplet). However, the P1 *myo*-Ins chemical shifts indicated that the *myo*-Ins was acylated on C-3. This was apparent from the H-3 deshielding (Δδ +1.36 ppm compared with the one in P3 *myo*-Ins (δ 3.24)). We

<sup>3</sup> B. Monsarrat, T. Brando, J. Nigou, M. Gilleron, and G. Puzo, unpublished data.

FIG. 4. Electrophoregram of APTS derivatives isolated from the H37Rv parietal ManLAMs mild hydrolysis (0.1 N HCl at 110 °C 30 min) and derivatization with APTS. A, Ara-APTS; G, Glc-APTS; M, Man-APTS; A-A, Araf-Ara-APTS; M-A, Manp-Ara-APTS; M-M-A, Manp-Manp-Ara-APTS; M-M-M-A, Manp-Manp-Manp-Ara-APTS. Peaks labeled with asterisks (\*) arise from the reagent.



were unable, however, to attribute the *myo*-Ins and Gro spin systems corresponding to P2 due to the weak representation of this population.

From these data, it can be proposed that P1 typified an anchor comprising a diacylated Gro and a *myo*-Ins acylated on C-3, while P3 characterized an anchor formed by a diacylated

Gro and a non-acylated *myo*-Ins. Although the P5 signal was weak, we were able to deduce the absence of an acyl residue on the C2 of the Gro, as no cross-peak was seen with a methine group around 5.10 ppm (Fig. 7a). In comparison to a standard, a *L*- $\alpha$ -lysophosphatidylinositol dissolved in Me<sub>2</sub>SO-*d*<sub>6</sub> (1-acyl-2-lyso-*sn*-glycero-3-phospho-(1-D-*myo*-inositol),  $\delta_{H-1/H-1'}$  3.99/3.97,  $\delta_{H-2}$  3.75,  $\delta_{H3/H3'}$  3.78/3.76), the Gro <sup>1</sup>H chemical shifts (Table II) indicated that the Gro was monoacylated on C1. Moreover, from the chemical shifts of the *myo*-Ins protons (Table II), the absence of fatty acyl appendage on the *myo*-Ins unit was deduced. P2 characterized an anchor comprising a 1-acyl-2-lyso-Gro and a non-acylated *myo*-Ins.

In summary, the major acyl-form of the parietal and cellular H37Rv ManLAMs, typified by the P3 resonance, comprises a diacyl-Gro unit (Fig. 8). In the case of cellular ManLAMs, mono- and triacylated forms of the anchor were also characterized. However, this NMR approach failed to identify a putative fatty acid on the C-6 of the Manp unit linked to the C-2 of the *myo*-Ins (32).

In order to determine the nature of the acyl groups present on the glycerol moiety, ManLAMs were submitted to acetolysis cleaving the phosphate glycerol linkage, but preserving the acylglycerol residues (20). These residues, extracted by cyclohexane/water partition, were analyzed by GC/MS in electron impact and chemical ionization/NH<sub>3</sub> ionization modes, as described previously (9). The diacylated Gro was assigned to 1-tuberculostearoyl-2-palmitoyl-*sn*-Gro, while the lyso-Gro forms correspond to both 1-palmitoyl-*sn*-Gro and 1-tuberculostearoyl-*sn*-Gro.

#### DISCUSSION

To survive in its human reservoir, *M. tuberculosis* has evolved molecular strategies to control both innate and acquired immune responses. The survival of *M. tuberculosis* within the alveolar macrophages, a hostile environment, hinges on immunosuppressive molecules. The infected host cells also sense the presence of mycobacteria from mycobacterial molecules that they recognize as foreign. This complex interplay between mycobacteria and hosts is mediated, on the one hand, by certain molecules, such those of the mycobacterial cell envelope, and on the other hand, by the activation of immune cells by the production of anti-microbial factors such as opsonins, peptides, cytokines, and chemokines.

Among the envelope molecules, LAMs are unique lipoglycans of the *Mycobacterium* genus and are considered as the major mycobacterial antigens (1). LAMs from pathogenic strains such as *M. tuberculosis*, *Mycobacterium leprae*, and the vaccine

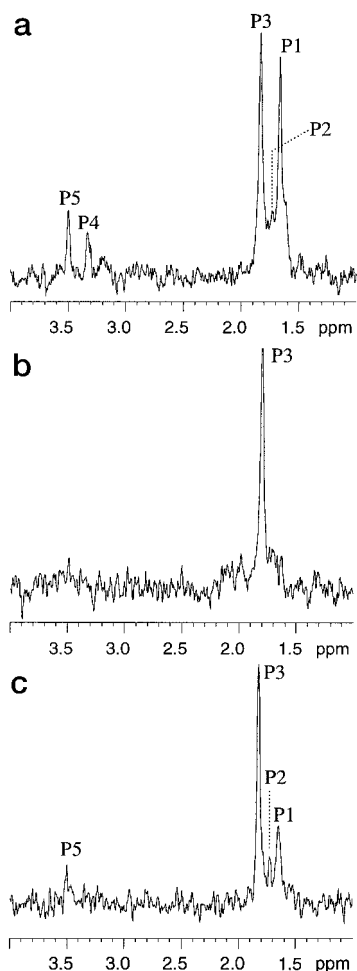


FIG. 5. One-dimensional <sup>31</sup>P spectra ( $\delta$  <sup>31</sup>P, 1.00–4.00) of cellular ManLAMs of *M. bovis* BCG (a) and parietal (b) and cellular (c) ManLAMs of *M. tuberculosis* H37Rv dissolved in Me<sub>2</sub>SO-*d*<sub>6</sub> at 343 K.

FIG. 6. NMR anchor analysis of parietal ManLAMs in Me<sub>2</sub>SO-*d*<sub>6</sub> at 343 K. a, expanded region ( $\delta$  <sup>1</sup>H, 3.00–5.30; and <sup>31</sup>P, 1.0–2.8) of the <sup>31</sup>P-decoupled, <sup>1</sup>H-detected 53 ms HMQC-HOHAHA spectrum. b, expanded region ( $\delta$  <sup>1</sup>H, 3.00–5.30; and <sup>31</sup>P, 0.9–2.7) of the <sup>31</sup>P-decoupled, <sup>1</sup>H-detected HMQC spectrum. Numerals correspond to the proton number of the *myo*-Ins unit and numerals with letter G, to the proton number of the glycerol unit.

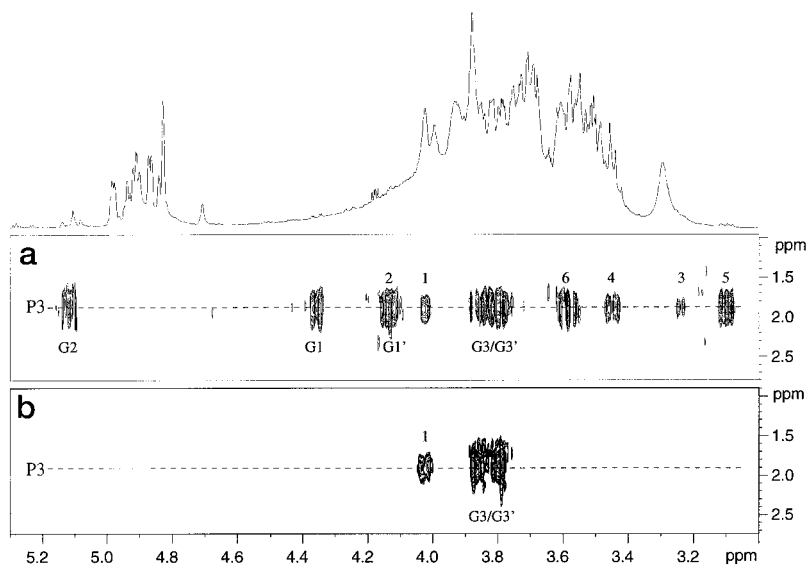


FIG. 7. NMR anchor analysis of cellular ManLAMs in  $\text{Me}_2\text{SO}-d_6$  at 343 K. *a*, expanded region ( $\delta^1\text{H}$ , 3.00–5.30; and  $^{31}\text{P}$ , 0.5–4.5) of the  $^{31}\text{P}$ -decoupled,  $^1\text{H}$ -detected 53 ms HMQC-HOHAHA spectrum; *b*, expanded region ( $\delta^1\text{H}$ , 3.00–5.30; and  $^{31}\text{P}$ , 0.5–4.5) of the  $^{31}\text{P}$ -decoupled,  $^1\text{H}$ -detected HMQC spectrum; *c*, expanded zone of the two-dimensional HOHAHA ( $\delta^1\text{H}$ , 3.00–5.30 and 2.95–3.40) spectrum showing the *myo*-Ins spin systems; *d*, expanded zone of the two-dimensional HOHAHA ( $\delta^1\text{H}$ , 3.00–5.30 and 4.25–4.50) spectrum showing the Gro spin systems. Numerals correspond to the proton number of the *myo*-Ins unit and numerals with letter G, to the proton number of the glycerol unit.

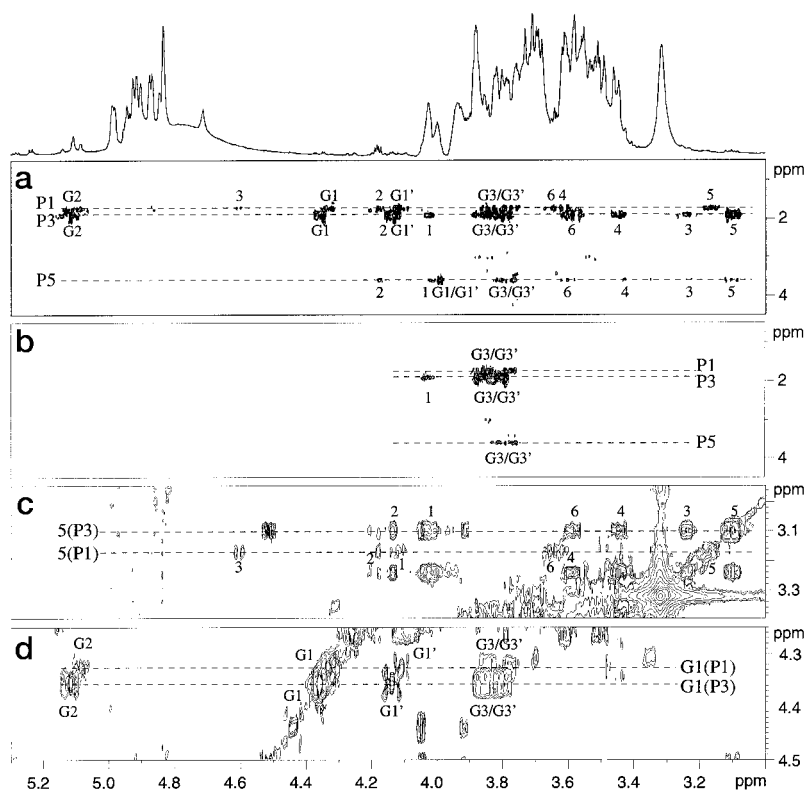


TABLE II

*P1/P3/P5 Gro and myo-Ins*  $^1\text{H}$  chemical shifts of cellular ManLAMs in  $\text{Me}_2\text{SO}-d_6$  at 343 K

	<i>myo</i> -Ins						Gro		
	H-1	H-2	H-3	H-4	H-5	H-6	H-1/H-1'	H-2	H-3/H-3'
P1	4.12	4.19	4.60	3.63	3.18	3.66	4.33/4.12	5.09	3.83/3.78
P3	4.03	4.13	3.24	3.46	3.11	3.59	4.37/4.15	5.12	3.85/3.81
P5	4.02	4.18	3.23	3.43	3.11	3.60	3.99/ND <sup>a</sup>	ND	3.81/3.77

<sup>a</sup> ND, not determined.

strain *M. bovis* BCG belong to the ManLAM class. ManLAMs are multifaceted molecules. They have been shown to be involved in the immunopathogenesis of tuberculosis as immunosuppressive molecules (2). Moreover, they are described as antigens of host double negative  $\alpha\beta$  T-cells (33). These T-cells secrete antibacterial peptides and interferon- $\gamma$  and may be involved in protective immunity. Delimitation of ManLAMs epitopes require knowledge of the precise structure of the ManLAMs. To date, the ManLAMs from BCG, *M. leprae*, and *M. tuberculosis* share the same structural model typified by the tripartite structure of a heteropolysaccharide of D-mannan and D-arabinan, a phosphatidyl-*myo*-inositol mannosyl anchor and the Manp caps (1, 34). In addition, some decorative residues, such as succinyl units, have been located on the arabinan domain (17). It is now established that ManLAMs from any single source are heterogeneous in size with respect to arabinan and mannan domains and degree of acylation (1, 9, 28). Unfortunately, the marked heterogeneity of ManLAMs hampers establishment of direct structure-function relationships.

Using the extraction procedure previously applied on *M. bovis* BCG (9, 17), the present report revealed the presence of two pools of ManLAMs, namely parietal and cellular, in the envelope of *M. tuberculosis* H37Rv. The location of these two pools of ManLAMs in the envelope of mycobacteria remains an open question. We surmised that the cellular ManLAMs were anchored in the plasma membrane as depicted by the envelope architecture proposed by Brennan *et al.* (35), while the parietal

ManLAMs are incorporated in the outer layer with other amphipatic molecules as phosphatidyl-*myo*-inositol mannosides, LMs, and glycolipids, as depicted by the envelope model proposed by Rastogi *et al.* (36). Using this new extraction procedure, significant amounts of AMs and LMs were also found in both cellular and parietal extracts of *M. tuberculosis* H37Rv and *M. bovis* BCG envelopes. In summary, two pools of molecules (including LAMs, LMs, and AMs) were identified, which were extracted according to their location in the mycobacterial envelopes. However, it should be borne in mind the topology of these pools will probably be modulated by interactions with the mycobacterial environment.

A recent study on ManAMs demonstrated that parietal and cellular ManAMs share a structural model assigned to ManLAMs devoid of the phosphatidyl-*myo*-Ins anchor (30). Although these two molecules are structurally very similar, they have quite different immunological functions. These ManAMs, but not ManLAMs, have also been found in culture medium (37). It may be that ManAMs arise from ManLAMs after action of an endogenous mycobacterial glycosylphosphatidylinositol phospholipase-like as described for glycosylphosphatidylinositol-anchored proteins (38). However, the excreted ManAMs could also arise from the traffic of cellular ManAMs through the envelope.

The Manp caps seem to play a major role in ManLAM activity, such as their binding to the mannose receptor (12, 13), and probably also in the recognition of ManLAMs by the  $\alpha\beta$  T cell receptor. By capillary electrophoresis, we found that both *M. tuberculosis* H37Rv parietal and cellular ManLAMs share the same cap structures assigned to Manp, Man $\alpha$ 1 $\rightarrow$ 2Manp, and Man $\alpha$ 1 $\rightarrow$ 2Man $\alpha$ 1 $\rightarrow$ 2Manp units. The Man $\alpha$ 1 $\rightarrow$ 2Manp motif corresponds to the major one as in the ManLAMs from *M. bovis* BCG (9).

The structure of the phosphatidyl-*myo*-Ins anchors of *M. tuberculosis* H37Rv parietal and cellular ManLAMs was established using one-dimensional  $^{31}\text{P}$  and two-dimensional  $^1\text{H}$ - $^{31}\text{P}$  NMR. The same populations of anchors as those described for

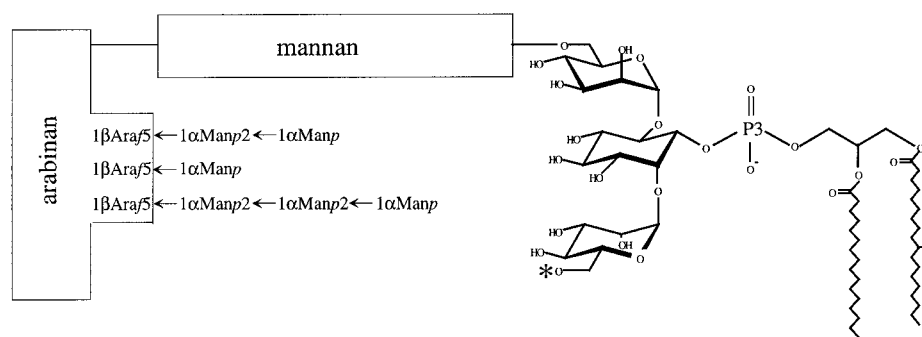


FIG. 8. Structural model of the major acyl-form of the anchor of the H37Rv parietal and cellular ManLAMs. The presence of a fatty acid (\*) on the Manp unit was not investigated in this study but is suggested by LAM degradative studies (32). The structures of the manno-oligosaccharide caps present at the nonreducing end of the arabinan domain arise from the capillary electrophoresis study. The dimannosyl unit represented 66%, while the mannosyl and trimannosyl represented 18 and 16%, respectively.

TABLE III  
Relative abundance (%) of phosphates of the different acyl-form populations

% of phosphate were given from peak heights on  $^{31}\text{P}$  NMR spectra. P2 was disregarded as it is not intense and unresolved. The acyl-form described for the parietal ManLAM from BCG (9) was tentatively assigned to P5 as it corresponds to a lyso-Gro and no fatty acid was observed on *myo*Ins unit.

		Diacylglycerol			Monoacylglycerol		
		P1	P3	P1 + P3	P4	P5	P4 + P5
H37Rv parietal ManLAMs	(88 mg)		100%	100%			0
H37Rv cellular ManLAMs	(140 mg)	22%	67%	89%		11%	11%
<b>H37Rv ManLAMs pool</b>	<b>(228mg)</b>	<b>13%</b>	<b>80%</b>	<b>93%</b>		<b>7%</b>	<b>7%</b>
BCG parietal ManLAMs	(23 mg)			0		100%	100%
BCG cellular ManLAMs	(255 mg)	38%	42%	80%	8%	12%	20%
<b>BCG ManLAMs pool</b>	<b>(278mg)</b>	<b>35%</b>	<b>39%</b>	<b>74%</b>	<b>7%</b>	<b>19%</b>	<b>26%</b>

cellular *M. bovis* BCG ManLAMs (28) were found in cellular H37Rv ManLAMs, but with different relative abundance (Table III). In cellular BCG ManLAMs, the  $^{31}\text{P}$  resonance were divided into two groups according to their chemical shifts. The first group composed of P1, P2, and P3 (resonating around 1.8 ppm) corresponds to phosphates esterifying diacylated Gro units. The second group, which contains P4 and P5 (observed at lower fields around 3.5 ppm), corresponds to phosphates esterifying 1-acyl-2-lyso-Gro units. In the case of *M. bovis* BCG, cellular ManLAMs with diacyl-Gro units represent approximately 80%, and 38% (P1) being acylated on the C-3 of the *myo*-Ins (Table III). The remaining 20% (P4 + P5) of ManLAMs contain 1-acyl-2-lyso-Gro units, 8% (P4) being acylated on the C-3 of the *myo*-Ins. In the case of *M. tuberculosis* H37Rv, cellular ManLAMs with diacyl-Gro forms represent 89%, P3 being the most represented population (67%) and P1 being less abundant than in BCG (22%). For both species, parietal ManLAMs are composed by a single acyl-form, corresponding to P3 for H37Rv and typified by a 1-(12-*O*-(methoxypropanoyl)-12-hydroxy-stearoyl)-*sn*-glycerol for BCG (9). Taken together, these data indicate that the acyl-forms are more heterogeneous in the cellular than in the parietal ManLAMs. In summary, the major anchor structure of H37Rv ManLAM pool, typified by the P3 resonance, is at least a diacylated anchor (80%) (Fig. 8). In the case of BCG, the major ManLAM anchors, typified by P1 and P3 resonance, are at least tri- (35%) and di- (39%) acylated anchors.

The fatty acyl appendage on the D-Manp linked to the C-2 of the *myo*-Ins residue described by Khoo *et al.* (32) could not be identified by the  $^{31}\text{P}$  NMR approach. We surmised that P1 typified a tetraacylated anchor (28), while the triacylated structure described by Khoo *et al.* (32) was represented by P2 or P3. Working on the total ManLAM pool, it is not possible to establish which acyl-form contains a fatty acid on the Manp. The definitive anchor structural determination with respect to the number of fatty acids will thus have to await purification of

each acyl-form followed by mass spectrometric analyses.

Finally, *M. tuberculosis* ManLAMs have been found to stimulate human double negative  $\alpha\beta$  T-cells restricted by CD1b molecules (39). Moreover, it has been established that the CD1 glycoproteins bind the ManLAMs through hydrophobic interactions via the fatty acid residues of the anchor moiety (40). The molecular pathway can be subdivided in three main steps: (i) the ManLAM uptake by the mannose receptor expressed on antigen presenting cell membranes, (ii) the ManLAM binding to the hydrophobic CD1b groove, and (iii) the ManLAM recognition by specific T cell receptors (33). Moreover, an  $\alpha\beta$ T-cell line (LDN4) was described proliferating in response to *M. leprae* ManLAMs but did not respond to that from *M. tuberculosis* (14), suggesting ManLAMs structural differences. However, to date, these ManLAMs share the same structural model. Indeed, a precise structural ManLAM characterization is complex as ManLAMs are composed of a large number of glyco- and acyl-forms. Characterization of *M. tuberculosis* ManLAMs acyl-forms should further understanding of the molecular mechanisms of ManLAM binding to the CD1 proteins involved in the presentation of ManLAMs to  $\alpha\beta$ T-cell receptors.

#### REFERENCES

- Chatterjee, D., and Khoo, K. H. (1998) *Glycobiology* **8**, 113–120
- Vercellone, A., Nigou, J., and Puzo, G. (1998) *Front. Biosci.* **3**, e149–163
- Sibley, L. D., Hunter, S. W., Brennan, P. J., and Krahenbuhl, J. L. (1988) *Infect. Immun.* **56**, 1232–1236
- Barnes, P. F., Chatterjee, D., Abrams, J. S., Lu, S., Wang, E., Yamamura, M., Brennan, P. J., and Modlin, R. L. (1992) *J. Immunol.* **149**, 541–547
- Roach, T. I., Barton, C. H., Chatterjee, D., and Blackwell, J. M. (1993) *J. Immunol.* **150**, 1886–1896
- Zhang, Y., Broser, M., Cohen, H., Bodkin, M., Law, K., Reibman, J., and Rom, W. N. (1995) *J. Clin. Invest.* **95**, 586–592
- Gilleron, M., Himoudi, N., Adam, O., Constant, P., Venisse, A., Riviere, M., and Puzo, G. (1997) *J. Biol. Chem.* **272**, 117–124
- Yoshida, A., and Koide, Y. (1997) *Infect. Immun.* **65**, 1953–1955
- Nigou, J., Gilleron, M., Cahuzac, B., Bounéry, J. D., Herold, M., Thurnher, M., and Puzo, G. (1997) *J. Biol. Chem.* **272**, 23094–23103
- Riedel, D. D., and Kaufmann, S. H. (1997) *Infect. Immun.* **65**, 4620–4623
- Chan, J., Fan, X. D., Hunter, S. W., Brennan, P. J., and Bloom, B. R. (1991) *Infect. Immun.* **59**, 1755–1761

12. Schlesinger, L. S., Hull, S. R., and Kaufman, T. M. (1994) *J. Immunol.* **152**, 4070–4079
13. Venisse, A., Fourmié, J. J., and Puzo, G. (1995) *Eur. J. Biochem.* **231**, 440–447
14. Sieling, P. A., Chatterjee, D., Porcelli, S. A., Prigozy, T. I., Mazzaccaro, R. J., Soriano, T., Bloom, B. R., Brenner, M. B., Kronenberg, M., Brennan, P. J., and Modlin, R. L. (1995) *Science* **269**, 227–230
15. Chatterjee, D., Hunter, S. W., McNeil, M., and Brennan, P. J. (1992) *J. Biol. Chem.* **267**, 6228–6233
16. Venisse, A., Berjeaud, J. M., Chaurand, P., Gilleron, M., and Puzo, G. (1993) *J. Biol. Chem.* **268**, 12401–12411
17. Delmas, C., Gilleron, M., Brando, T., Vercellone, A., Gheorghui, M., Rivière, M., and Puzo, G. (1997) *Glycobiology* **7**, 811–817
18. Prinzi, S., Chatterjee, D., and Brennan, P. J. (1993) *J. Gen. Microbiol.* **139**, 2649–2658
19. Khoo, K. H., Dell, A., Morris, H. R., Brennan, P. J., and Chatterjee, D. (1995) *J. Biol. Chem.* **270**, 12380–12389
20. Ferguson, M. A., Haldar, K., and Cross, G. A. (1985) *J. Biol. Chem.* **260**, 4963–4968
21. Guttman, A., Chen, F. T., Evangelista, R. A., and Cooke, N. (1996) *Anal. Biochem.* **233**, 234–242
22. Marion, D., and Wuthrich, K. (1983) *Biochem. Biophys. Res. Commun.* **113**, 967–974
23. Bax, A., and Davis, D. G. (1985) *J. Magn. Res.* **65**, 355–360
24. Bax, A., and Subramanian, S. (1986) *J. Magn. Reson.* **67**, 565–569
25. Shaka, A. J., Barker, P. B., and Freeman, R. (1985) *J. Magn. Res.* **64**, 547–552
26. Lerner, L., and Bax, A. (1986) *J. Magn. Reson.* **69**, 375–380
27. Delmas, C., Venisse, A., Vercellone, A., Gilleron, M., Albigot, R., Brando, T., Rivière, M., and Puzo, G. (1997) in *Techniques in Glycobiology* (Townsend, R. R., and Hotchkiss, A. T. J., eds) pp. 85–109, Marcel Dekker, Inc., New York
28. Nigou, J., Gilleron, M., and Puzo, G. (1999) *Biochem. J.* **337**, 453–460
29. Gilleron, M., Nigou, J., Cahuzac, B., and Puzo, G. (1998) *J. Mol. Biol.* **285**, 2147–2160
30. Nigou, J., Gilleron, M., Brando, T., Vercellone, A., and Puzo, G. (1999) *Glycoconj. J.* **16**, 257–264
31. Monsarrat, B., Brando, T., Condouret, P., Nigou, J., and Puzo, G. (1999) *Glycobiology* **9**, 335–342
32. Khoo, K. H., Dell, A., Morris, H. R., Brennan, P. J., and Chatterjee, D. (1995) *Glycobiology* **5**, 117–127
33. Prigozy, T. I., Sieling, P. A., Clemens, D., Stewart, P. L., Behar, S. M., Porcelli, S. A., Brenner, M. B., Modlin, R. L., and Kronenberg, M. (1997) *Immunity* **6**, 187–197
34. Gilleron, M., Rivière, M., and Puzo, G. (1999) in *Glycans in Cell Interaction and Recognition: Therapeutic aspects* (Aubery, M., ed) Harwood Academic Publishers, Amsterdam, in press
35. Brennan, P. J. (1989) *Rev. Infect. Dis.* **11**, S420–430
36. Rastogi, N. (1991) *Res. Microbiol.* **142**, 464–476
37. Lemassu, A., and Daffé, M. (1994) *Biochem. J.* **297**, 351–357
38. McConville, M. J., and Ferguson, M. A. (1993) *Biochem. J.* **294**, 305–324
39. Porcelli, S. A. (1995) *Adv. Immunol.* **59**, 1–98
40. Zeng, Z., Castano, A. R., Segelke, B. W., Stura, E. A., Peterson, P. A., and Wilson, I. A. (1997) *Science* **277**, 339–345